J Nanostruct 15(4): 2535-2552, Autumn 2025

RESEARCH PAPER

Adsorption and Photocatalysis of Biosynthesis ZnO–MgO Nanocomposite for Removing Malachite Green Dye from Their Aqueous Solutions

*Zainab H. Mohammed [1], Hanadi A. Fadhil [2], Khaled. W. Shuker [1], Juman A. Naser [2] **

[1] *Ministry of Education, Baghdad, Iraq*

[2] *Department of Chemistry, College of Education for Pure Science-Ibn Alhaitham, University of Baghdad, Baghdad, Iraq*

ARTICLE INFO

Article History:
Received 05 June 2025
Accepted 27 September 2025
Published 01 October 2025

Keywords:
Adsorption
Green synthesis
Malachite green
Photocatalysis
Wastewater treatment
ZnO–MgO nanocomposite

ABSTRACT

In this work, a green-synthesised ZnO–MgO nanocomposite made from orange peel extract is used to study the synergistic adsorption and UV-assisted photocatalytic degradation of malachite green (MG) dye from aqueous solutions. X-ray diffraction (XRD), scanning electron microscopy (SEM), and Fourier transform infrared spectroscopy (FTIR) were used to exchange data regarding the structure, chemistry, and form of the nanocomposite. Several operational parameters, such as adsorbent dosage, contact time, initial dye concentration, temperature, and UV irradiation conditions, were used to assess a removal performance in a batch system. Experimental results indicated that the ZnO–MgO nanocomposite had improved adsorption effectiveness under optimum circumstances, however the combined UV-photocatalytic process markedly increased the degradation of MG compared to adsorption alone. The Langmuir isotherm model suited the data for equilibrium better. This suggests that there was one layer of adsorption on a flat surface. Negative ΔG° results showed that the elimination process is spontaneous and possible, which was supported by thermodynamic characteristics. Studies on regeneration and reusability showed that the ZnO–MgO nanocomposite maintained its high removal effectiveness across several cycles. After being washed, dried, and reactivated with UV light several times, the material still had most of its ability to adsorb and photocatalyze. The fact that it is stable means that the composite is good for the economy and can be used for a long time. The material is very recyclable because it is strong, keeps active surface sites, and does not rust when exposed to UV light. The green-synthesized ZnO–MgO nanocomposite was very good at getting rid of malachite green dye by using both adsorption and UV photocatalysis. It could be a long-lasting and cost-effective material for advanced wastewater treatment because it has a lot of activity, is stable, and can be used again.

How to cite this article
Mohammed Z., Fadhil H., Shuker K., Naser J. Adsorption and Photocatalysis of Biosynthesis ZnO–MgO Nanocomposite for Removing Malachite Green Dye from Their Aqueous Solutions. J Nanostruct, 2025; 15(4):2535-2552. DOI: 10.22052/JNS.2025.04.089

* *Corresponding Author Email: juman.a.n@ihcoedu.uobaghdad.edu.iq*

INTRODUCTION

Synthetic organic pollutants, particularly those that originate from industries, are making water pollution a growing and bigger hazard to the health of people and the environment across the globe [1]. Synthetic dyes are one of the biggest pollutants since these are utilized in a lot of various places, such leather, paper, textiles, and plastic. Most typical treatments don't work on them very well because of this. Recent estimates show that the textile sector alone releases a lot of untreated dyes into water systems. This implies the need to look for therapeutic methods that function effectively and endure a long time [3]. Malachite green (MG) is one of the most dangerous colors since it is very poisonous and is used in many places [4]. This triphenylmethane dye is not allowed in many places, but it is nevertheless used in aquaculture and certain other sectors since it is cheap and works well [5]. Recent studies have shown that MG is more detrimental than previously believed; it may induce cancer and mutations, and even little quantities may disrupt the endocrine system [6]. It is very important and essential to get rid of it from industrial waste water since it is very hard to break down and stays stable in water for a long time. For a long time, there have been many different approaches to clean up wastewater. These include of chemical methods (such as enhanced oxidation and coagulation), physical methods (such as filtration and sedimentation), and biological methods [8].

But these approaches don't always work effectively for getting rid of MG and other complicated chemical substances. these may also be expensive and create a lot of sludge or other harmful by-products [9]. For this reason, adsorption has turned out to be one of the best, most flexible, and most scalable ways to treat anything [10]. It is simple to use, not too costly, may be used again, and can get rid of extremely little levels of contaminants [11]. It is highly vital to produce novel adsorbent materials that have a wide surface area, the proper amount of porosity, a lot of them, and are affordable [12]. Nanotechnology has made a big difference in how therapeutic materials are made [13]. Nanomaterials have made it easier to get rid of contaminants from the environment and break them down chemically than previous materials. This is because nanomaterials have special traits, such extremely tiny particles, a very large surface area, and a high surface reactivity [14]. Researchers have studied a range of nanomaterials, such as nano-activated carbons, nanoclays, metal–organic frameworks (MOFs), and metal oxide nanoparticles [15]. Metal oxide nanoparticles are one of the most fascinating kinds of nanoparticles. These are simple to find, have a lot of different chemical characteristics, are stable at high temperatures and pressures, and their surfaces are easy to modify [16]. Metal oxide nanoparticles clean water in two main ways: by sticking to pollutants and use light to break them down [17]. Nanoparticles of zinc oxide (ZnO) have excellent adhesion properties and the ability to neutralize reactive oxygen species (ROS) [18], rendering toxic organic molecules inert.

Magnesium oxide nanoparticles (MgO), however, are inexpensive, have a lot of surface area, and are known to be low in toxicity and have antibacterial capabilities [19]. When these two oxides are combined to produce a ZnO/MgO nanocomposite, these work together to make a stronger material. MgO may assist ZnO nanoparticles spread out and block electron-hole pairs generated by light from recombining via mutual doping. This makes it easier for molecules to stick to surfaces and lets photocatalytic activity happen in the visible light spectrum [20]. Nanomaterials have a lot of promise, but manufacturing them the old-fashioned manner (with chemicals and physical methods) generally involves toxic substances, unpleasant working conditions, and a lot of wasted energy, which is bad for the environment and goes against the tenets of green chemistry [21]. That's why making nanomaterials from plant extracts is now a long-lasting and good for the environment choice [22]. This approach employs plant extracts that include bioactive chemicals such polyphenols, flavonoids, and alkaloids that function as natural stabilizers and reducers. This makes it possible to make nanoparticles in only one step [23].

This work used orange peel extract, a prevalent and cost-effective agricultural by-product, as a green agent for the synthesis of the ZnO/MgO nanocomposite. Orange peels include flavonoids including hesperidin and naringin, as well as vitamin C. These are effective in lowering and stabilizing things on their own [24]. In this instance, prior research has diligently endeavored to use plant extracts for the fabrication of nanomaterials intended for water purification. For instance, research [25] employed mint leaf

extract to produce zinc oxide nanoparticles and then investigated how well these acted as photocatalysts to break down malachite green when these were exposed to UV light. The findings indicated that 94% of the material could be broken down in 120 minutes. This indicates how effective green synthesis approaches may be. This research concentrated only on one kind of metal nanomaterial and did not investigate the synergistic effects of nanocomposites. It also only worked under UV light, which makes it less effective for huge projects. Researchers in [26] made a hybrid SnO_2/ZnO nanocomposite using pomegranate peel extract as a reducing agent, which is similar to a recent discovery. In this investigation, the elimination of the hue methylene blue was the primary objective. The adsorption rate of 96% demonstrated that the nanocomposite outperformed its constituent elements in this regard. The findings demonstrated that the photocatalytic activity was enhanced due to the simplified separation of charges caused by the interaction of the two oxides. The research only focused on adsorption analysis and employed a multi-step preparation approach. The elimination of the very poisonous malachite green or photocatalysis were not addressed. By developing a green synthesis of a ZnO/MgO nanocomposite using orange peel extract and assessing its capacity to remove malachite green dye using a hybrid approach that includes adsorption and photocatalysis under simulated sunshine, this work creates a significant gap in the literature. Contrasted with other research, this one has more merit. This study breaks new ground as it replaces conventional chemical procedures with orange peel extract to create a binary oxide nanocomposite (ZnO/MgO). Aside from being a photocatalyst for ZnO, it has the ability to absorb large amounts of MgO.

The primary objective of this research was to determine the efficacy of an environmentally friendly zinc oxide/magnesium oxide nanocomposite made from orange peel extract in removing the green hue of malachite from water. In order to create and examine the nanocomposite, this research aims to employ sophisticated analytical instruments such as FTIR, XRD, and SEM. We may have a better understanding of its form and structure from this. Additionally, it must be aware of the optimal means of removal and the nanocomposite's performance in various contexts as an adsorbent and photocatalyst. The study goal is to clarify the process of elimination by looking at adsorption isotherm models and testing photocatalytic activity in conditions that mimic sunlight.

MATERIALS AND METHODS

Chemicals

Chemicals were very pure and came from trustworthy sources for this work. The main precursor salts were magnesium sulfate heptahydrate ($MgSO_4 \cdot 7H_2O$) and zinc sulfate heptahydrate ($ZnSO_4 \cdot 7H_2O$). Both were bought from Sigma–Aldrich (USA) and were at least 99% pure. Merck (Germany) sent sodium hydroxide pellets (NaOH) that were used to make a 1.0 M precipitating solution. Distilled water was used for all the steps of preparation and washing to make sure that the process was clean and that impurities didn't get in the way. The plant extract was freshly prepared locally from bitter orange (Citrus aurantium) peels without the addition of any other chemicals, and it served as a reducing and stabilizing agent in the green synthesis[27] of the MgO–ZnO nanocomposite.

Green Synthesis of the MgO–ZnO Nanocomposite

The MgO–ZnO nanocomposite was synthesized using a green approach in which bitter orange (Citrus aurantium) peel extract served as both a reducing and stabilizing agent for nanoparticle formation. Initially, fresh orange peels were thoroughly washed, air-dried, and finely ground. To get phenolic compounds, flavonoids, and natural sugars out of the powdered peels, 10 g of them were boiled in 200 mL of distilled water for 20 minutes. These are bioactive compounds that are known to be very important for reducing and stabilizing metal nanoparticles. Further processing included filtering the heated extract through standard filter paper and storing it at 4 °C until needed.

Characterization of Adsorbent

Analyzing the physicochemical features of the produced MgO-ZnO nanocomposite using a range of characterization methods allowed us to understand its elemental makeup, crystalline structure, and surface characteristics. For the first time, Field Emission Scanning Electron Microscopy (FESEM) was used to investigate the shape, arrangement, and dispersion of surface

particles, their adhesion mechanisms, and the dimensions of structures at the nanoscale. Investigations using Energy-Dispersive X-ray Spectroscopy (EDS) uncovered the components and their even distribution. Zinc, magnesium, and oxygen were the most abundant elements found in the EDS spectra. There were also trace levels of carbon in the plant extract that was used in the green synthesis process. Using Fourier Transform Infrared Spectroscopy (FT-IR), we were able to analyze the bitter orange peel extract for phytochemicals and the nanocomposite for surface functional groups. These plant compounds had a dual role as stabilizers and reductants. The FT-IR data also showed the evolution of the Zn-O and Mg-O vibrational modes. Using X-ray diffraction (XRD) analysis, which involves looking for diffraction peaks associated with magnesium oxide and zinc oxide, the crystalline phases of the nanocomposite were found. By using the Scherrer equation to better understand the size of the crystallites, gained a better understanding of the material's nanoscale characteristics. This complete characterization technique allowed us to understand the surface and structural features of the MgO-ZnO nanocomposite. It also clarified the material's superior performance in photocatalytic and adsorption settings.

Adsorption Experiments

The malachite green hue was removed using batch-based adsorption and photocatalytic experiments conducted in a shaking incubator (HYSC SWB-25, Korea). Incubator stirring at a constant 120 rpm maintained nanocomposite distribution and excellent contact throughout the experiment. The test solutions were consistently 50 mL in volume and included dye concentrations of 20, 30, 40, 50, and 60 mg/L. The MgO-ZnO nanocomposite, which weighed just 0.03 g, was the key ingredient. The same adjusted contact time was used for both adsorption and photocatalysis. No test was performed at a temperature lower than 25 °C. After the liquid settled after the adsorption experiments, centrifugation was used to separate the components. To provide the best possible catalytic conditions for the photocatalytic testing, the reaction mixture was agitated continuously

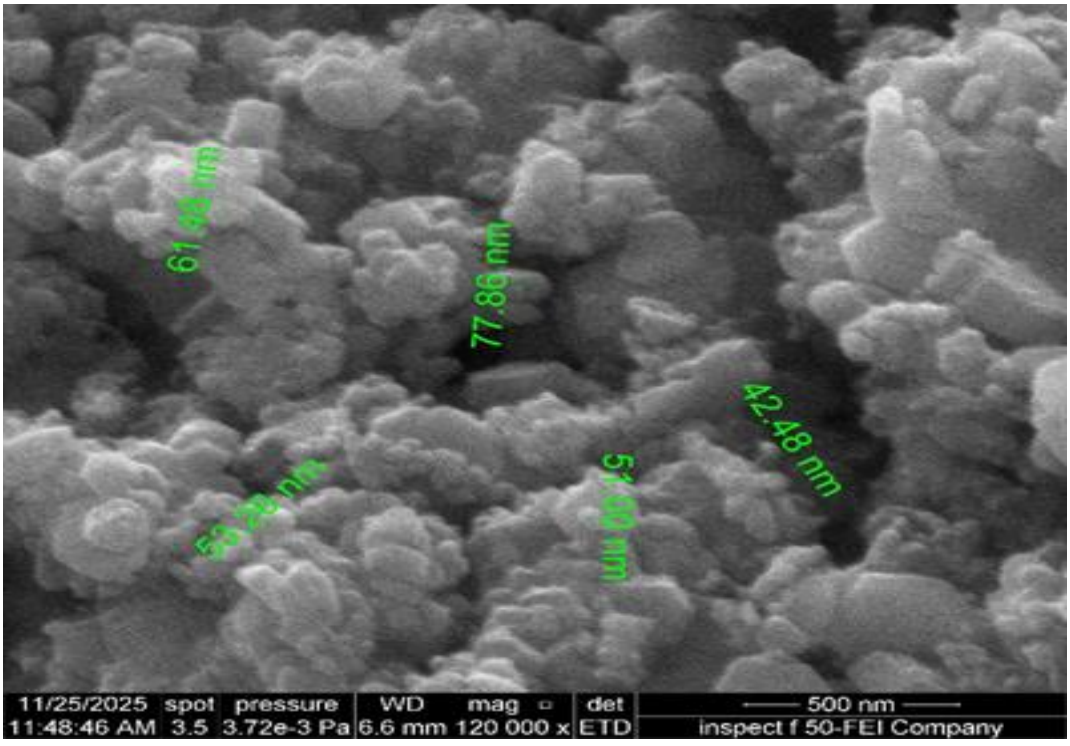

Fig. 1. FESEM Image for MgO–ZnO Nanocomposite.

while being exposed to the appropriate light source.

The absorbance of the remaining dye at the maximum wavelength of malachite green was measured using a UV-Vis spectrophotometer. Because of this, we were able to more easily gauge the amount of color remaining in the combination. Using established formulae, the adsorption capacity and the removal have determined. The studies were carried out under carefully controlled settings to guarantee the reliability of the findings and to allow for the comparison of the photocatalytic and adsorption activities at all the different dosages that were tested.

Factors Affecting Adsorption

Many essential operating aspects to get the green-synthesized MgO–ZnO nanocomposite made from bitter orange peel extract perform better. Each parameter has examined individually, ensuring that all other variables remained constant. At first, looked at how varied quantities of adsorbent, from 0.01 g to 0.05 g, changed the removal performance by looking at how much active surface area was available. We collected samples every 15, 30, 45, 60, 75, 90, and 105 minutes to see how long it took for the two things to reach equilibrium. In addition, to look at how the starting amount of malachite green changed the way it was removed from water that was more or less dirty. Values ranging from 20 to 60 mg/L were analyzed for this purpose. We tested at 298, 303, 313, and 323 K to examine how temperature and heat change the performance of adsorption and photocatalysis. After each experiment, the nanocomposite was washed and dried, and then it was used again in a fresh adsorption cycle under the same conditions to see whether it could be reused (regenerated). The test demonstrated that the material's structure and chemistry are stable and that it can remain performing well after many cycles. This is a good hint that it might operate well in real-world environmental systems.

Concentration Determining

After each experiment, a centrifuge was used to separate the adsorbent from the solution. The centrifuge spun at 6000 rpm for 10 minutes to make sure that all of the nanomaterial was removed from the water. UV–Vis was used spectrophotometer to measure the remaining amount of Malachite Green in the filtrate at its highest absorption wavelength of 617 nm. A standard equations are often used in adsorption

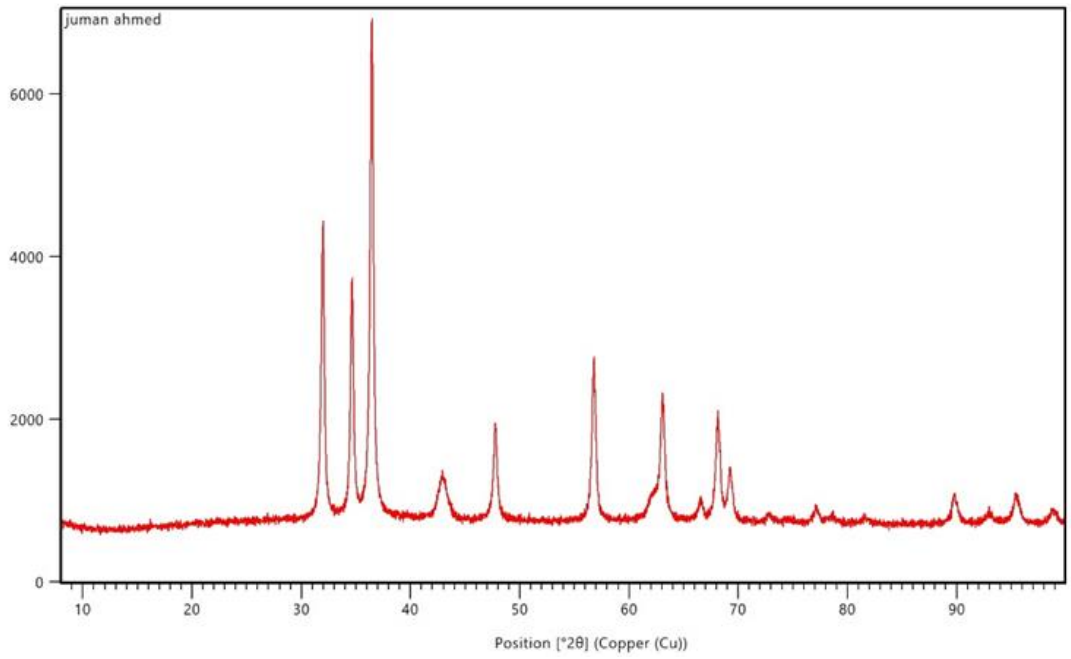

Fig. 2. XRD Spectrum of MgO–ZnO Nanocomposite.

studies to figure out the adsorption capacity (q_e) and the removal efficiency, q_e (mg/g) [28]:

$$q_e = \frac{(C_o - C_e)V}{m} \quad \textbf{(1)}$$

Here, C_e stands for ion concentration at equilibrium (mg/L), C_o stands for initial ion concentration (mg/L), m stands for mass of adsorbent (g) and V is the volume of salt solution (L).

RESULTS AND DISCUSSION

Characterization of Adsorbent

A successful synthesis for MgO–ZnO nanocomposite prepared using natural bitter orange peel extract has been confirmed by comprehensive characterization techniques.

Scanning Electron Microscopy (SEM)

The biosynthesized MgO–ZnO nanocomposite's FESEM images showed an agglomerated and highly irregular morphology made up of clustered nanoparticles with heterogeneous grain sizes ranging roughly between 40 and 80 nm (Fig. 1). The formation of interconnected nanoscale structures was indicated by the surface's rough and closely packed appearance. This morphology points to a successful green synthesis using bitter orange peel extract, where the phytochemicals serve as capping and stabilizing agents [29]. This results in the formation of compact nano-aggregates with a large number of active surface sites that are appropriate for photocatalytic reactions and adsorption.

X-ray Diffraction Spectroscopy (XRD)

The X-ray diffraction pattern of the green-synthesized MgO–ZnO nanocomposite exhibited a series of sharp and intense peaks, confirming its well-defined crystalline structure (Fig. 2). The characteristic reflections observed at 2θ values of 31°, 34°, 36°, 47°, 56°, 62°, and 68° correspond to the hexagonal wurtzite phase of ZnO, in accordance with the standard JCPDS data[30]. Additional peaks appearing near 2θ ≈ 43° and 62° are attributed to the cubic phase of MgO, indicating the coexistence of both oxide phases within the composite.

Fourier Transform Infrared (FTIR)

The FTIR spectrum of the green-synthesized MgO–ZnO nanocomposite prepared using bitter orange peel extract confirms the successful formation of the material and the presence of phytochemical species on its surface. A broad absorption band at 3435 cm^{-1} corresponds to O–H

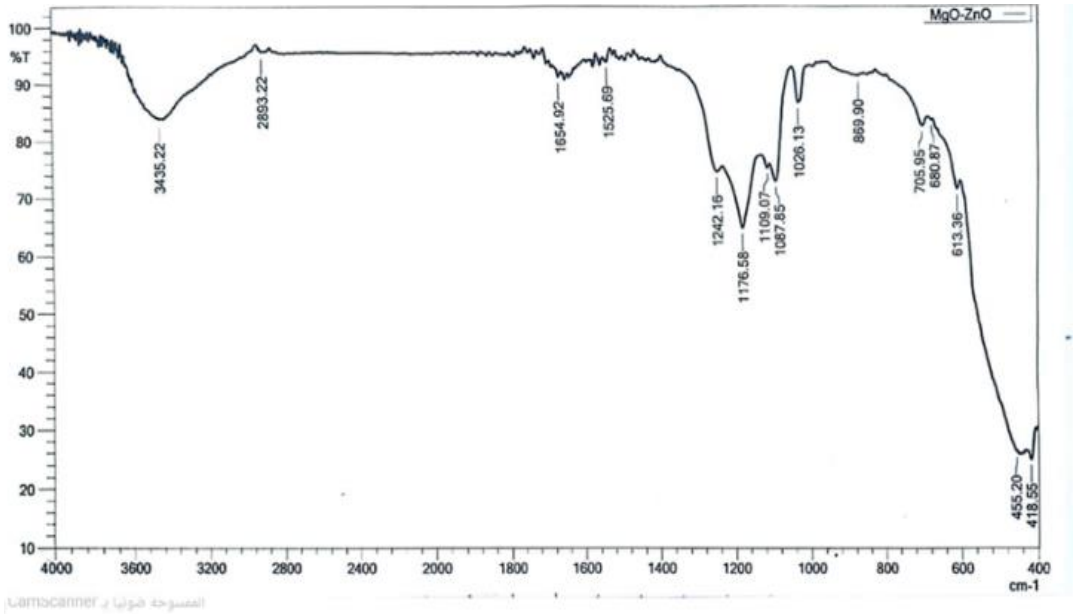

Fig. 3. FTIR Spectrum of MgO–ZnO Nanocomposite.

stretching vibrations, originating from surface hydroxyl groups or residual phenolic compounds from the plant extract, indicating extensive hydrogen bonding.

The peak observed near 2883 cm^{-1} is attributed to C–H stretching vibrations of organic molecules involved in the green synthesis process. Pronounced absorptions at 1654 and 1525 cm^{-1} correspond to C=O and C=C vibrations from polyphenols and carboxyl-containing compounds present in the extract[31], confirming their role as stabilizing and capping agents for the nanoparticles.

Additional bands in the region 1242–1109–1026 cm^{-1} are associated with C–O and C–O–C vibrations, reflecting the presence of natural polysaccharides and oxygenated functional groups from the extract. Characteristic metal–oxygen vibrations appear in the lower region of the spectrum: bands at 705–680–613 cm^{-1} correspond to Zn–O stretching, while the strong band at 455 cm^{-1} confirms the presence of Mg–O, characteristic of magnesium oxide.

Overall, the FTIR results demonstrate the successful biosynthesis of the MgO–ZnO nanocomposite and verify the interaction of the extract's phytochemicals with the metal oxide surface, enhancing stability and providing active sites for adsorption and photocatalytic applications.

Energy Dispersive X-ray Spectroscopy (EDS)

The EDS spectrum recorded for the MgO–ZnO nanocomposite (Fig. 4), together with the corresponding quantitative data (Table 1), confirms the elemental composition of the biosynthesized material. A spectrum depicts strong signals for Zn and Mg, as well as clear peaks for O. This means

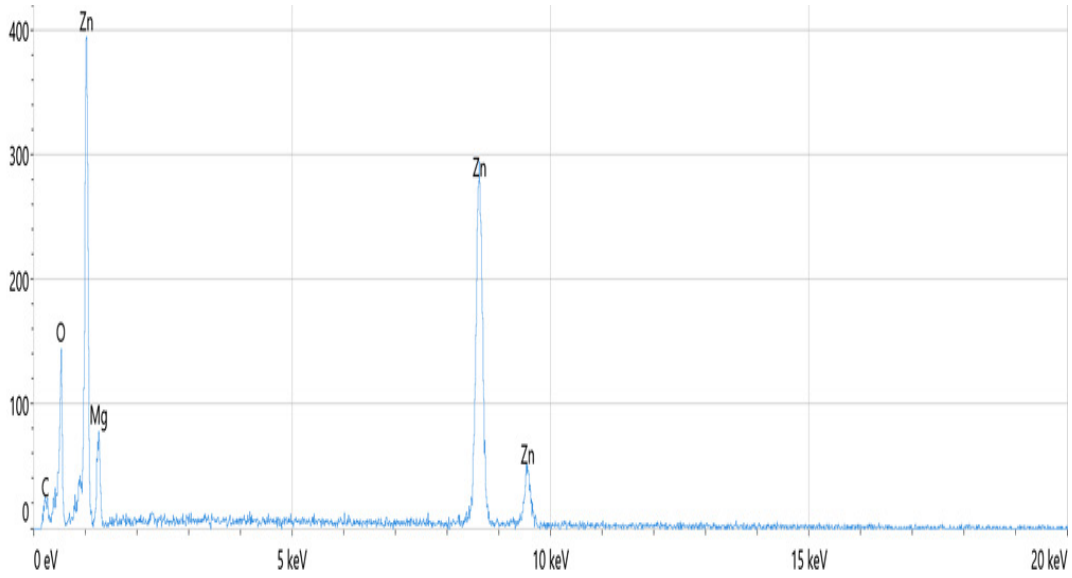

Fig. 4. EDS Spectrum of MgO–ZnO Nanocomposite.

Table 1. Elemental Composition of MgO–ZnO Nanocomposite.

Element	Atomic %	Atomic % Error	Weight %	Weight % Error
C	17.3	3.2	6.5	1.2
O	35.6	1.6	17.9	0.8
Mg	16.3	0.6	12.5	0.5
S	0.5	0.1	0.5	0.1
Zn	30.4	0.8	62.6	1.6

that zinc, magnesium, and oxygen are the main parts of the composite. Zinc makes up about 30.4 at.% (62.6 wt.%), and magnesium makes up 16.3 at.% (12.5 wt.%), which is in line with the idea that a ZnO–MgO mixed oxide system is forming instead of a simple physical mixture. The relatively high oxygen content (35.6 at.%) supports the idea that metal oxides have metal-oxygen bonds.

A noticeable amount of carbon (17.3 at.% and 6.5 wt.%) is also detected, which can be attributed to organic residues originating from the bitter orange peel extract used as a green reducing and stabilizing agent during synthesis, as well as to the carbon coating applied during SEM sample preparation. The very low percentage of sulfur (0.5 at.% and wt.%) likely arises from trace components in the plant extract and does not indicate the presence of a separate sulfur-containing phase.

Overall, the dominance of Zn, Mg and O together with the absence of any additional metallic elements in the EDS profile confirms the successful preparation of a chemically pure MgO–ZnO nanocomposite, while the detected carbon signal supports the proposed green synthesis mechanism involving phytochemicals adsorbed on the nanoparticle surface.

Calibration Curve of Malachite Green

A calibration curve for Malachite Green was constructed over the concentration range of 0–60 mg/L, showing a highly linear relationship between absorbance and concentration. The experimental data fit the straight line Eq. 2 with a coefficient of determination of $R^2 = 0.9976$:

$$A = 0.0293\ C + 0.0224 \quad \textbf{(2)}$$

This means that the measured values and the linear model were very similar and agreed with each other very well. This high R^2 value shows that the spectrophotometric measurements are accurate and that this calibration curve can be used to find the equilibrium concentrations (Ce) from the measured absorbance values. The positive slope of the calibration curve shows that the dye follows the Beer–Lambert law in the concentration range looked at. This means that absorbance goes up in a straight line with concentration, with no signs of saturation or spectral deviation. So, you can be sure that you can use this calibration curve for all the calculations you do later to find out the adsorption capacity (Qe) and removal efficiency

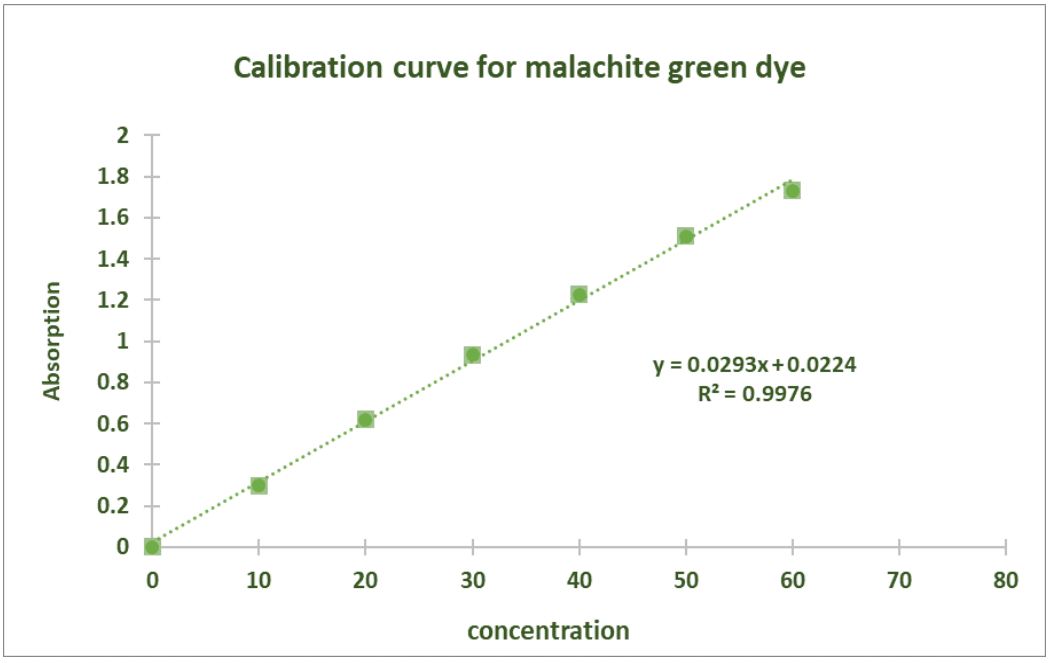

Fig. 5. Calibration Curve for Malachite Green Dye.

during the experiments.

Factors Affecting Adsorption

Effect of Adsorbent Dose

Fig. 6 shows how the amount of MgO–ZnO adsorbent affects how well it removes Malachite Green dye. The results show that increasing the dose from 0.01 to 0.03 g made it much easier to remove the dye. The improvement is due to the fact that adding more adsorbent particles to the system increases the number of active surface sites that can be used for adsorption. However, giving more than 0.03 g did not significantly improve the removal efficiency. At higher doses (0.04–0.05 g), the adsorption capacity (qe, mg/g) went down a little. This could be because not all of the adsorption sites were used up and nanoparticles tend to clump together when these are too concentrated. This type of agglomeration makes the effective surface area smaller and makes it harder to get to active sites[32]. Based on these results, a dose of 0.03 g was chosen as the best amount because it was the best balance between getting rid of the most dye and using the least amount of material.

Effect of Contact Time

The effect of contact time on the adsorption of Malachite Green dye onto the MgO–ZnO nanocomposite was examined under optimized conditions (Fig. 7). The adsorption capacity increased rapidly during the first 45 minutes, which is attributed to the large number of available active sites on the surface of the nanocomposite. As time went on, the adsorption rate slowly dropped because these active sites were getting more and more full. The system got close to equilibrium after about 90 to 100 minutes, and after that, only small changes in adsorption capacity were seen. The first stage of fast adsorption is mostly caused by interactions between surfaces and diffusion from the outside. The second stage is mostly caused by diffusion between particles as dye molecules move deeper into the pores and surface irregularities of the MgO–ZnO nanostructure [33].

Effect of Initial Concentration

T looked at how the initial concentration of malachite green dye affected the MgO–ZnO adsorbent's ability to remove it and its catalytic form. The concentration range was 20–60 mg/L.

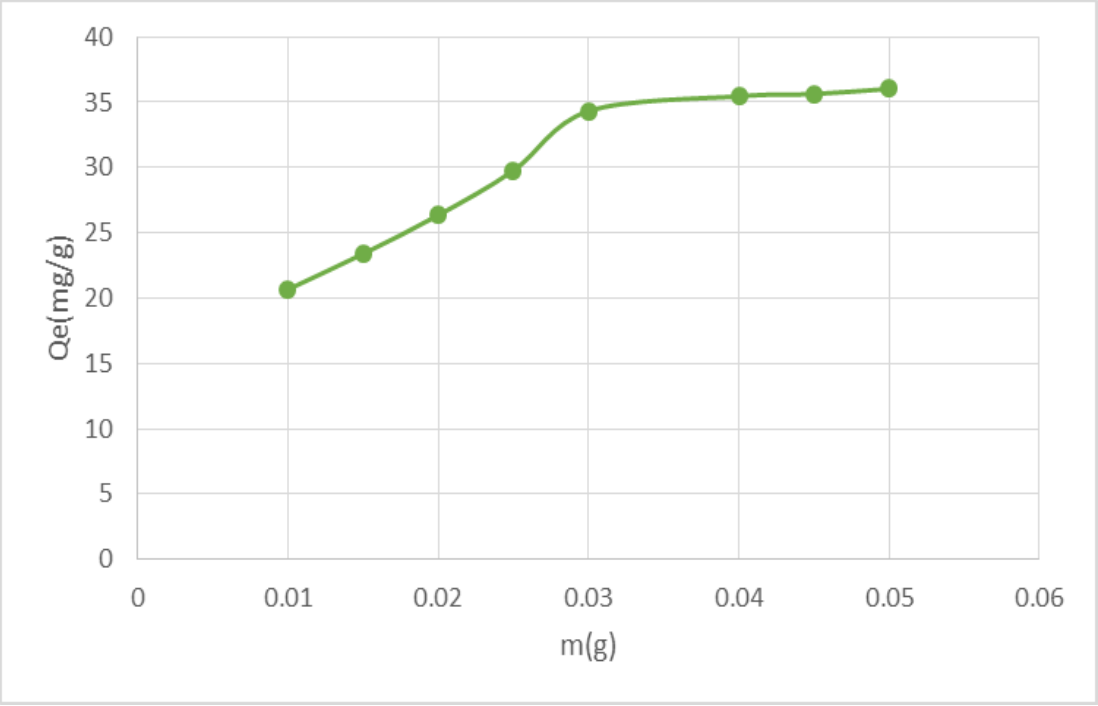

Fig. 6. Effect of Adsorbent Dose for Malachite Green Dye adsorption onto MgO–ZnO Nanocomposite.

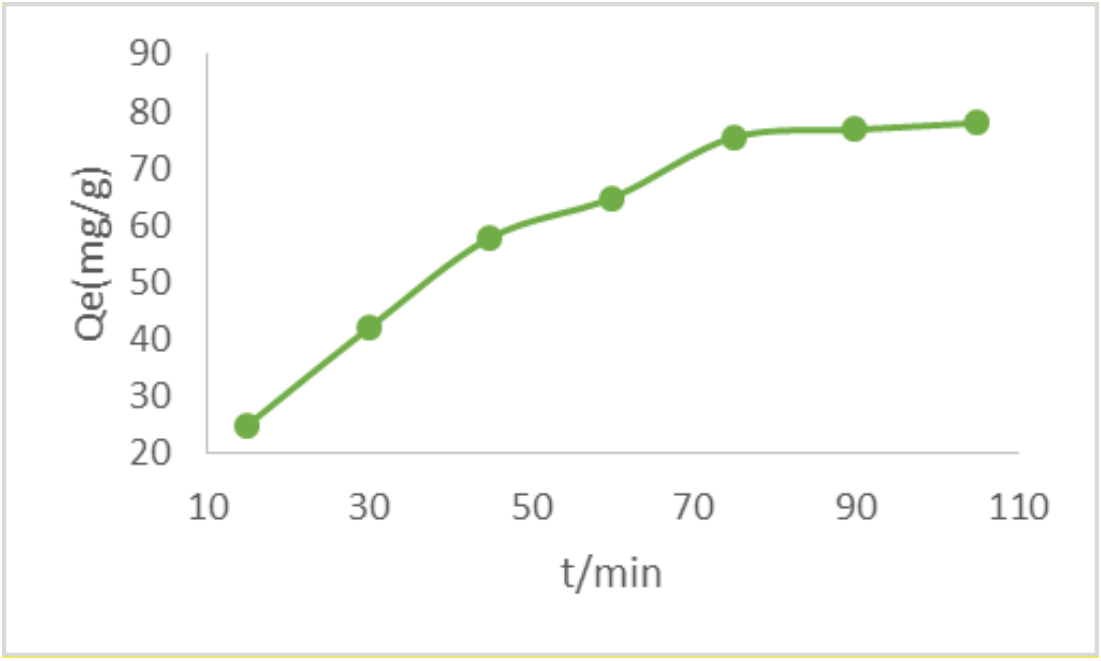

Fig. 7. Contact time effect for Malachite Green Dye adsorption onto MgO–ZnO Nanocomposite.

Fig. 8 shows that the removal percentage (%R) followed a pattern for both systems: %R went down at the middle concentrations because dye molecules were competing more for the few surface active sites available[34]. This shows that the surface was saturated. The elimination efficiency increased up again at greater concentrations (around 60 mg/L). This is because there were more collisions and a larger force pushing mass toward the surface of the adsorbent. Because the %R values were always highest at 323 K, temperature was a crucial factor. As a result, whereas adsorption often produces heat, higher temperatures aid dye mobility and surface dispersion. The catalytic system (Cat.) significantly outperformed the pure adsorption system (Ads) across the board in terms of %R, regardless of concentration or temperature. This is superior because it has catalytically active surface centers that improve dye interaction, decrease diffusion resistance, and maintain system performance in the presence of increased contaminants. These findings demonstrate that the adsorption-catalytic system is more stable at elevated temperatures and produces a superior surface for dye removal. This makes it an excellent option for places that produce a high volume of organic trash during cleanup.

Effect of Ionic Strength

The results show that when the ionic strength was raised with NaCl and KCl solutions, the adsorption capacity (Q_e) slowly went down, while the equilibrium concentration (C_e) went up a little. The electrostatic shielding effect[35] explains this behavior. The positive ions in the solution make the forces that pull the dye molecules and the active sites on the adsorbent's surface together weaker. There are more ions contending for space near the surface as the salt concentration rises. This makes the ionic layer congested, which makes it harder for dye molecules to get toward the active sites and increases the competition for these sites greater. It was also found that KCl stopped the reaction better than NaCl since it generated a greater reduction in Qe at the same doses. Due to their distinct ionic characteristics, the two salts are in fact distinct from one another. Sodium ions (Na^+) have a higher hydration energy and a smaller hydrated radius compared to potassium ions (K^+). This facilitates their approach to the adsorbent surface, where they may engage in competition with the dye molecules. The effectiveness of the adsorption process is further diminished by this.

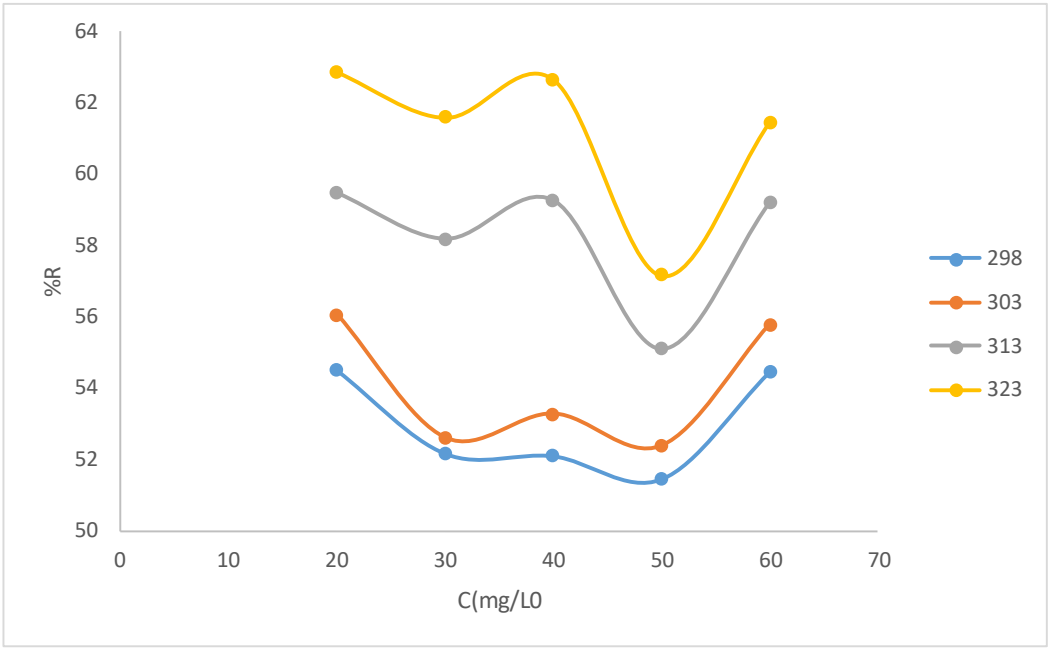

Fig. 8. Initial concentration effect for Malachite Green Dye adsorption onto MgO–ZnO Nanocomposite.

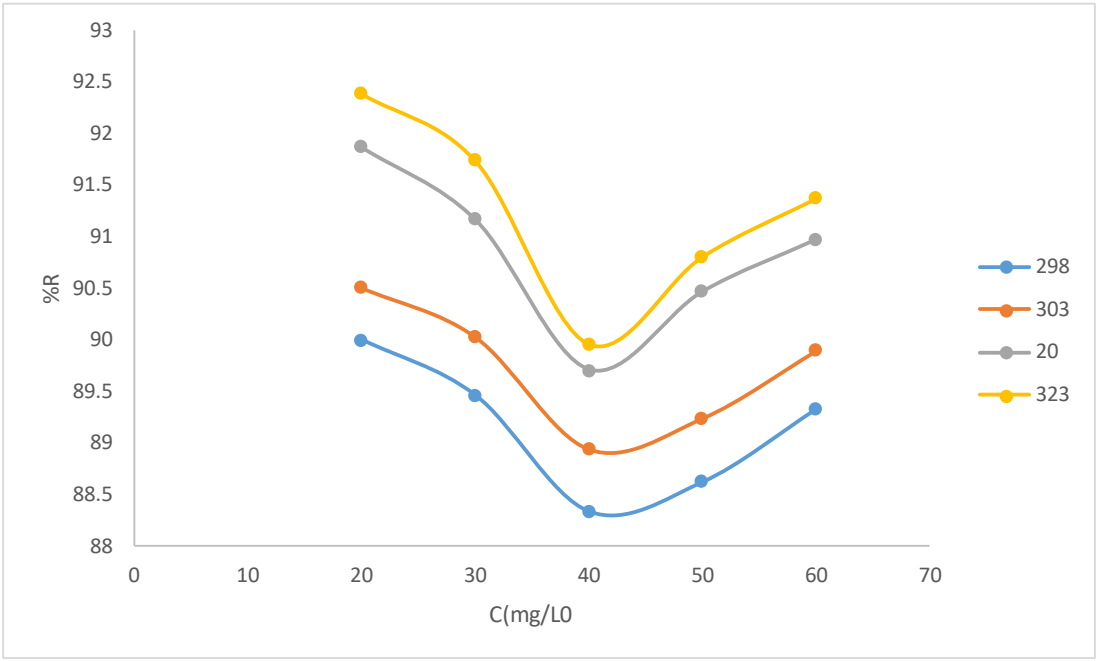

Fig. 9. Initial concentration effect for Malachite Green Dye adsorption onto MgO–ZnO Nanocomposite.

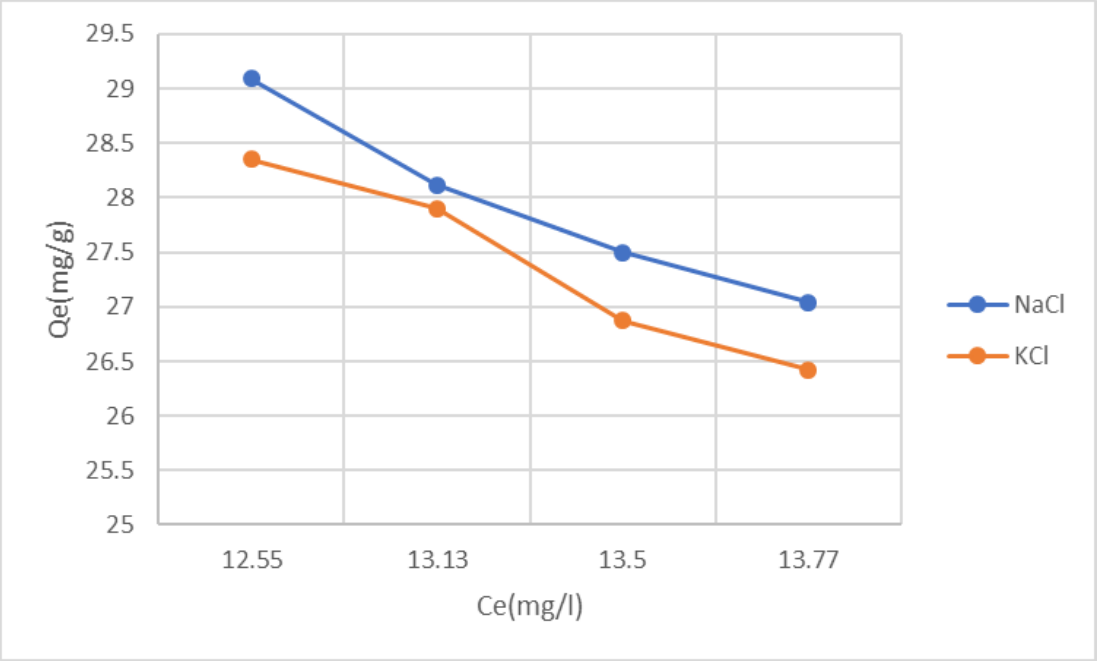

Fig. 10. Effect of Ionic Strength of Malachite Green Dye adsorption onto MgO–ZnO Nanocomposite.

Based on these findings, electrostatic interactions seem to be the main force behind the adsorption in the system under study. These connections get weaker with the addition of additional ions, making it more difficult to remove the dye. Sodium is less affected by this than potassium.

Regeneration and Reusability of Adsorbent

Regeneration experiments demonstrated that the adsorbent retained some adsorption capacity after one day of collection, washing, and drying. An increase in the equilibrium concentration (Ce) was accompanied by an increase in the adsorption capacity (Qe). The mended surface was able to perform many of the same functions as before. An increase in Ce from 20 to 60 mg/L caused a shift in Qe levels from 18.11 to 53.49 mg/g. Even as the concentration increases, Qe continues to rise. Thus, the regeneration process is effective, and the first adsorption cycle did not cause any harm or irreversible blocking of the active sites. This indicates that the regenerated surface functions similarly to the fresh adsorbent, as the curve is almost straight. This makes it resistant to chemicals as well as the heat generated during washing and drying.

These results show that the material can be used over and over again without losing much of its power. This is very important for businesses and the environment because it saves money and is good for the environment. So, the regenerated adsorbent can still be very useful in systems that treat things over and over again.

Adsorption Isotherms

To further understand the interaction of lead and cadmium ions with the surface of the adsorbent material, equilibrium data were analyzed using Langmuir and Freundlich models [36], as shown in Eqs. 3 and 4:

$$\frac{C_e}{q_e} = \frac{1}{q_{max} k_L} + \frac{C_e}{q_{max}} \quad (3)$$

where q_e is quantity of ions at equilibrium (mg/g), C_e is the concentration of ions (mg/L), q_{max} is the maximum capacity of adsorption and kL is Langmuir experimental constant.

Figs. 8 and 9 that produces the values of the Langmuir constants q_{max} and k_L is Ce/qe versus Ce. In this instance, the slope of the line represents q_{max}, while the intercept is k_L.

$$\ln q_e = \ln k_f + \frac{1}{n} \ln C_e \quad (4)$$

where q_e is the amount of adsorbed ions at equilibrium (mg/g), C_e is the adsorbed concentration of ions at equilibrium (mg/L), both k_f and n are experimental constants of Freundlich. kf and n have been calculated using the intercept and slope of a plot of lnqe vs. lnCe, Figs. 10 and 11.

The equilibrium adsorption data of malachite green dye onto MgO–ZnO nanocomposite were analyzed using both Langmuir and Freundlich isotherm models for the adsorption-only system (ads) and the catalytic/adsorptive system (cat). The results demonstrated that the Langmuir model provided a superior fit compared to the Freundlich model across most temperatures, as indicated by the higher correlation coefficients (R^2 ≈ 0.96–0.98 for ads, and 0.94–0.98 for cat). This strong agreement confirms that the removal of dye molecules occurs mainly through monolayer adsorption on a homogeneous surface with energetically uniform active sites.

In contrast, the Freundlich model showed significantly lower R^2 values, particularly for the adsorption-only system (R^2 ≈ 0.18–0.37), suggesting that multilayer adsorption or surface heterogeneity plays a minimal role. Regeneration experiments demonstrated that the adsorbent retained some adsorption capacity after one day of collection, washing, and drying. An increase in the equilibrium concentration (Ce) was accompanied by an increase in the adsorption capacity (Qe). The mended surface was able to perform many of the same functions as before. An increase in Ce from 20 to 60 mg/L caused a shift in Qe levels from 18.11 to 53.49 mg/g. Even as the concentration increases, Qe continues to rise. Thus, the regeneration process is effective, and the first adsorption cycle did not cause any harm or irreversible blocking of the active sites.

The curve is almost straight, which means that the regenerated surface works like the new adsorbent. This means that it can handle both chemicals and heat when it is washed and dried.

The catalytic system consistently outperformed the adsorption-only system at all temperatures, demonstrating more efficient dye removal due to the combined effects of surface adsorption and thermally assisted catalytic degradation. These results show that MgO–ZnO is a good dual-function material for treating wastewater that contains organic dye pollutants.

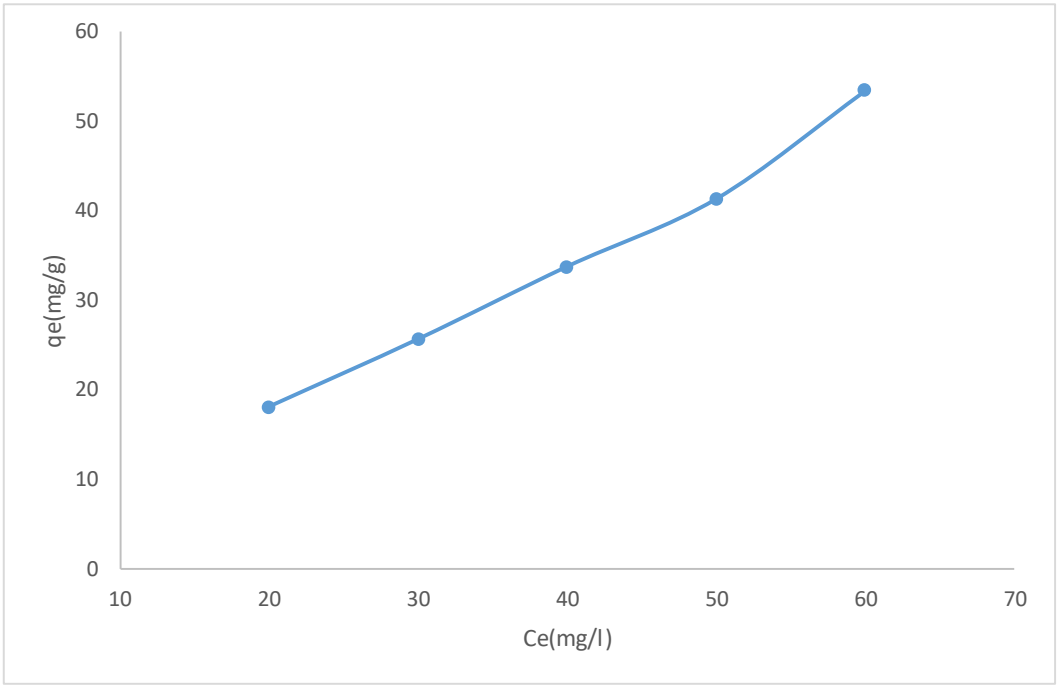

Fig. 11. Regeneration Efficiency of MgO–ZnO Nanocomposite over Successive Cycles.

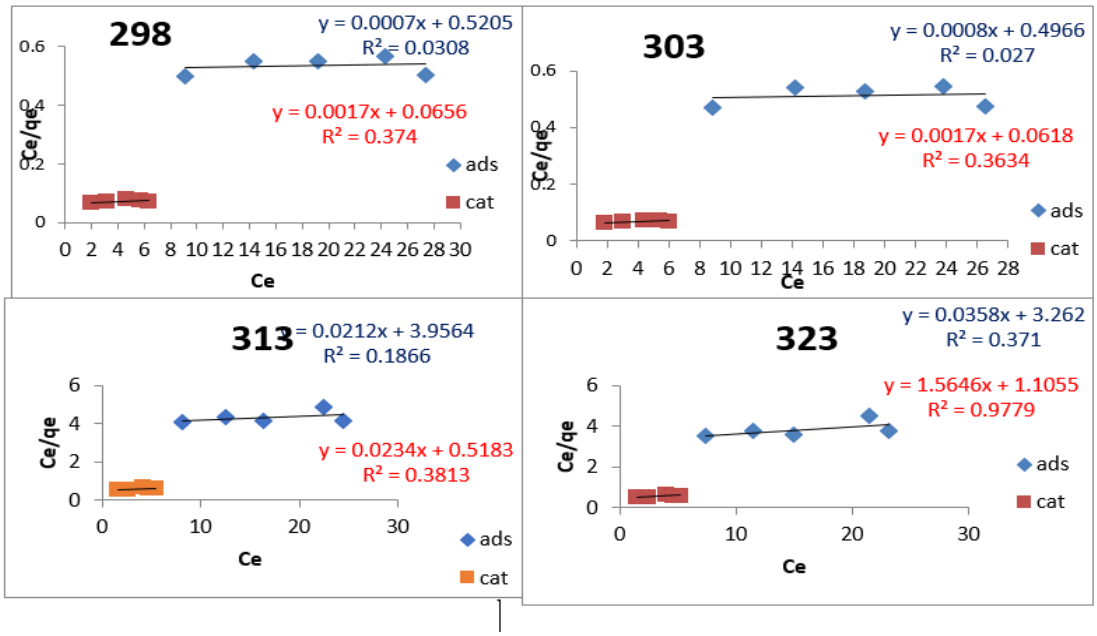

Fig. 12. Langmuir isotherms of Adsorption and Photocatalysis of Malachite Green Dye onto MgO–ZnO Nanocomposite.

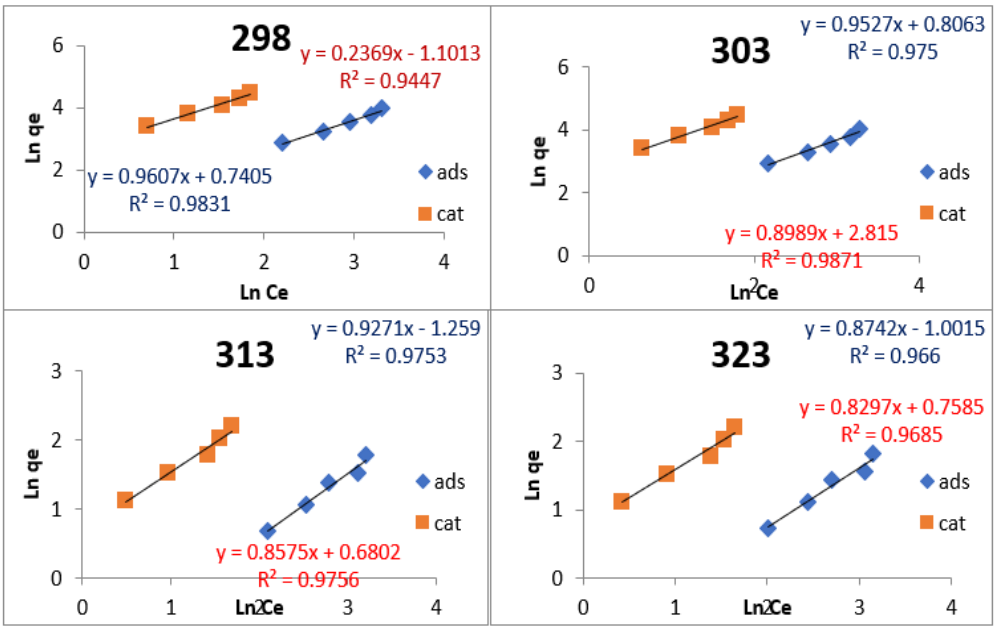

Fig. 13. Freundlich isotherms of Adsorption and Photocatalysis of Malachite Green Dye onto MgO–ZnO Nanocomposite.

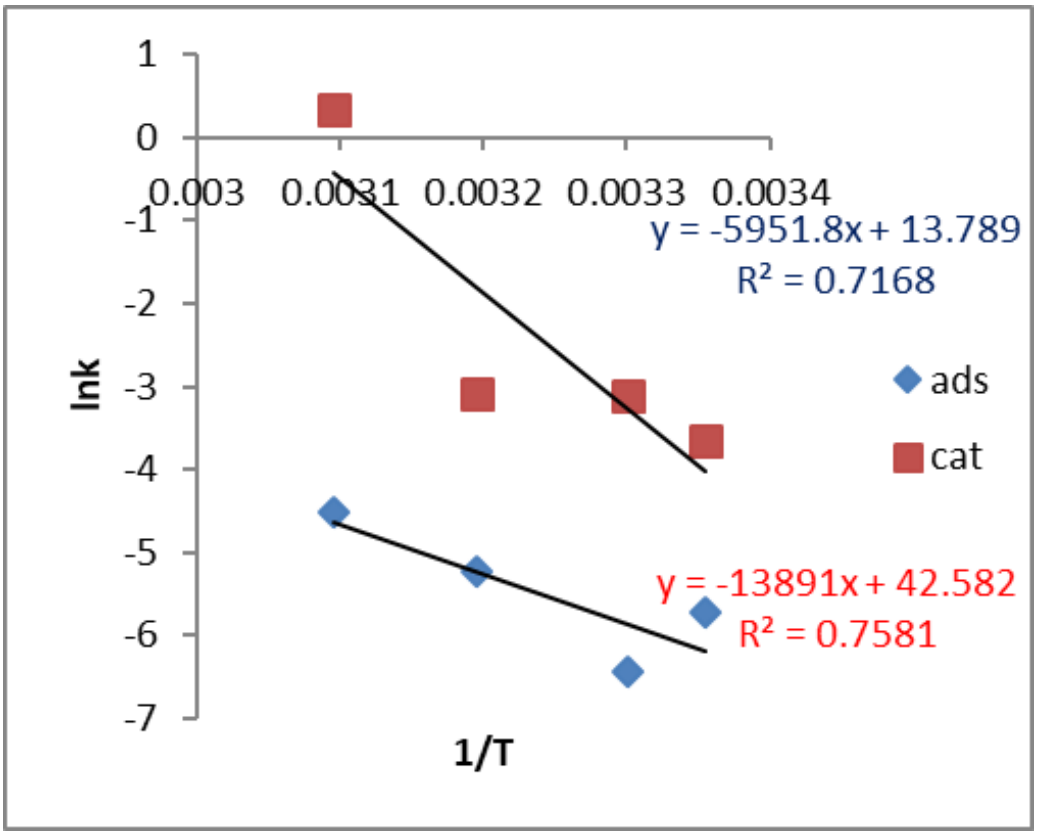

Fig. 14. Represents van't Hoff equation of Adsorption as well as Photocatalysis of Malachite Green Dye onto MgO–ZnO Nanocomposite.

Table 2. Values of Thermodynamic Functions forfor Malachite Green Dye Adsorption onto MgO–ZnO Nanocomposite.

Temperature (K)	ΔHº(kJ/mol)	ΔGº(kJ/mol)	ΔSº(J/mol.K)
298	-5951.8	-890.439	-16.9844
303		-2031.18	-12.9393
313		-3263.26	-8.58958
323		-2689.45	-10.1002

Table 3. Magnitudes for Thermodynamic Functions of Malachite Green Dye Photocatalysis onto MgO–ZnO Nanocomposite.

Temperature (K)	ΔHº(kJ/mol)	ΔGº(kJ/mol)	ΔSº(J/mol.K)
298	-13891	-2728.55	-37.4579
303		-6885.82	-23.1194
313		-1770.07	-38.725
323		-2036.89	-36.7

Thermodynamics of Adsorption

An effect for temperature on adsorption was investigated at 298, 308, and 318 K, Fig. 12. The thermodynamic functions were continuously calculated using the Eq. 5 [37]:

$$\ln K = \frac{-\Delta H}{RT} + \text{constant} \quad (5)$$

That equation uses Kelvin temperature unit (T), a universal gas constant (R), a thermodynamic equilibrium constant (K), and an enthalpy change for adsorption (ΔH). The slope of the straight line in Fig. 14, which is the outcome of plotting lnK against 1/T (van't Hoff plot), was used to calculate the enthalpy shift. An estimate of the free Gibbs energy, Go, was obtained using the Eq. 6 [38]:

$$\Delta G^0 = -RT\ln K \quad (6)$$

An equilibrium Gibbs formula has been employed for estimating entropy changes (ΔS°) (Eq. 7) [39]:

$$\Delta G^0 = \Delta H^0 - T\Delta S^0 \quad (7)$$

The thermodynamic parameters obtained from the Van't Hoff plots (ΔH°, ΔG°, and ΔS°) indicate that the adsorption of malachite green dye onto the MgO–ZnO composite primarily occurs via a physical adsorption mechanism. The negative enthalpy values (ΔH°) for both the adsorption and catalytic systems show that the process gives off heat [40]. This means that raising the temperature weakens the bond between the dye molecules and the surface, making it less effective at removing them. Gibbs free energy values (ΔG°) are always negative, which means that adsorption happens on its own at all of the temperatures studied. Small changes in these values suggest that certain thermal conditions make adsorption more favorable. Negative entropy values (ΔS°) depict that solid–liquid interface has been less random, which means that dye molecules are moving from the water medium to surface sites that are more ordered and stable in terms of energy. These observations suggest that adsorption is influenced by weak physical forces, primarily the electrostatic attraction between positively charged dye molecules and negatively charged surface groups on MgO–ZnO, as well as diffusion into nanoscale pores and secondary interactions, including dipole–dipole or van der Waals forces. The catalytic system (cat) works better because it has more active centers that speed up the movement of mass and the approach to equilibrium. The process is spontaneous, gives off heat, and is mostly controlled by physiosorption. This makes the material work well at low temperatures and makes it easy to regenerate and use again.

The MgO–ZnO composite removes malachite green dye primarily through electrostatic attraction between the negatively charged surface sites and the cationic dye molecules, according to the combined results of structural characterization, adsorption equilibrium, and thermodynamic analysis. The predominant role of physical adsorption within surface pores, supported by van der Waals and weak dipole–dipole interactions, lends credence to this. The process is confirmed to follow a physisorption mechanism instead of a chemisorption pathway by the low negative values of ΔH° and ΔG°.

CONCLUSION

In this study, Citrus aurantium (bitter orange) peel extract was used to create a green MgO–ZnO nanocomposite, which was successfully tested as an effective adsorbent and photocatalyst for the removal of malachite green dye from aqueous solutions. A mixed-oxide nanocomposite with a crystalline structure, lots of oxygenated functional groups, and a heterogeneous, rough, porous surface that offers a high density of active sites was successfully formed, according to the characterization analyses (FTIR, FESEM, XRD, and EDS). While EDS confirmed that the elemental composition was dominated by Zn (30.4 at%), Mg (16.3 at%), and oxygen-rich surface groups necessary for dye interaction, FESEM images showed nano-aggregates with particle sizes ranging from 42 to 78 nm. The nanocomposite shows high removal efficiency under ideal conditions, according to batch adsorption tests. The adsorption capacity went up a lot when the dye concentrations went from 20 to 60 mg/L, but the clearance % went down because the surface sites were full. The first absorption occurred immediately, according to experiments with contact time, and remained constant for around 90 to 100 minutes after that. This occurred for a couple of reasons: first, the film expanded, and second, the particles penetrated the internal

pores. Results showed that removal behavior changed between 298 and 323 K, according to the temperature investigation. At 323 K, the %R for the adsorption (ads) and catalytic (cat) systems were they maximum. This indicates that greater temperatures facilitate the mobility of dye molecules, even if the process is said to emit heat according to the thermodynamic characteristics. Both adsorption and catalytic systems show that the Freundlich model is not as effective as the Langmuir model, according to isotherm modeling. The fact that this occurs on a perfectly flat surface proves that monolayer adsorption occurs there. According to the thermodynamic data, the process is both exothermic ($\Delta H° < 0$) and spontaneous ($\Delta G° < 0$). When the color stays, the surface ordering improves, as shown by the negative $\Delta S°$ readings. In every case, the catalytic approach outperformed direct adsorption due to the increased number of reactive sites that accelerated the dye's degradation. As a result, removal rates and capacities increased. The surface's capacity to bind dye molecules decreased in the presence of NaCl and KCl, according to ionic strength tests. This proved that salt ions and color molecules were vying for the same physical location. The MgO-ZnO nanocomposite continues to absorb a great deal of material even after several cycles, according to regeneration research. Two major advantages for actual wastewater treatment are its stability and its reusability, both of which it has. According to the results, a sustainable MgO-ZnO nanocomposite is an excellent adsorbent-photocatalyst for large-scale remediation of organic dye-contaminated water systems since it is efficient, inexpensive, and harmless to the environment. With its high activity sites, robust thermodynamics, ease of recycling, and excellent catalytic properties, it is an excellent material for environmental cleanup methods.

CONFLICT OF INTEREST

The authors declare that there is no conflict of interests regarding the publication of this manuscript.

REFERENCES

1. Shi Y, Xing Y, Ma C, Sun Y, Ding G. Degradation of aqueous organic pollutants by dual oxidant advanced oxidation processes: A comprehensive review. Journal of Environmental Chemical Engineering. 2024;12(6):114174.
2. Singh A, Kishor R, Bharagava RN, Yadav BC. Existing and Emerging Treatment Technologies for the Degradation and Detoxification of Textile Industry Wastewater for the Environmental Safety. Bioremediation: CRC Press; 2022. p. 1-13.
3. Okeke ES, Ezeorba TPC, Chen Y, Mao G, Feng W, Wu X. Association of tetrabromobisphenol A (TBBPA) with micro/nano-plastics: A review of recent findings on ecotoxicological and health impacts. Sci Total Environ. 2024;927:172308.
4. Liu H, Lv H, Xu H, Rao D, Zhang J, Sun B. Is monochloramine pre-oxidation a viable strategy for enhancing the treatment efficiency of algae-laden water with conventional drinking water treatment process? Chemosphere. 2024;352:141312.
5. Al-Ghouti MA, Al-Absi RS. Mechanistic understanding of the adsorption and thermodynamic aspects of cationic methylene blue dye onto cellulosic olive stones biomass from wastewater. Sci Rep. 2020;10(1).
6. Payamifar S, Abdouss M, Poursattar Marjani A. Recent advances in β-cyclodextrin-based catalyst systems for the synthesis of heterocyclic compounds via multicomponent reactions (MCRs). Arabian Journal of Chemistry. 2024;17(10):105967.
7. Huang W, Zhou J, Liang Y, Saladin RJ, Li L, Kang L, et al. Applications of smart responsive nanomaterials in the theranostics of gastrointestinal malignancies: Current status and future perspectives. Coord Chem Rev. 2025;535:216641.
8. Li J, Wang S, Li R, Zhang B, Xu X, Wang Z, et al. Construction of Z-scheme photocatalyst with p-n heterojunction of molecular semiconductors for enhanced photocatalytic water oxidation. Applied Catalysis B: Environmental. 2024;342:123381.
9. Construction of gC3N4 Metal-Free Heterostructure Film for Enhanced Photocatalytic Degradation of Organic Pollutants. American Chemical Society (ACS). http://dx.doi.org/10.1021/acs.langmuir.5c01557.s001
10. Jadoun S, Arif R, Jangid NK, Meena RK. Green synthesis of nanoparticles using plant extracts: a review. Environ Chem Lett. 2020;19(1):355-374.
11. Varshney S, Gupta A. Forest industrial biomass residue-mediated green synthesized multifunctional copper oxide nanoparticles for efficient wastewater treatment and biomedical applications. Journal of Cleaner Production. 2024;434:140109.
12. Iqbal T, Afzal M, Al- Asbahi BA, Afsheen S, Maryam I, Mushtaq A, et al. Enhancing apple shelf life: A comparative analysis of photocatalytic activity in pure and manganese-doped ZnO nanoparticles. Mater Sci Semicond Process. 2024;173:108152.
13. Sudha D, Kumar ER, Shanjitha S, Munshi AM, Al-Hazmi GAA, El-Metwaly NM, et al. Structural, optical, morphological and electrochemical properties of ZnO and graphene oxide blended ZnO nanocomposites. Ceram Int. 2023;49(5):7284-7288.
14. Abduh NAY, Al-Kahtani A, Al-Odayni A-B. Phyto-mediated synthesis of ZnO nanoparticles and their sunlight-driven photocatalytic degradation of cationic and anionic dyes. Open Chemistry. 2024;22(1).
15. Green Nanotechnology for Water Remediation: Eco-Friendly Synthesis of Zinc Oxide Nanoparticles and Methylene Blue Degradation Kinetics. American Chemical Society (ACS).
16. Al-Juboori RA, Ahmed FE, Khanzada NK, Khatri M, Al-shaeli M, Ibrahim Y, et al. Burgeoning innovation and scalability activities for phosphorus recovery from wastewater treatment facilities. Sustainable Materials and Technologies. 2024;40:e00907.

17. Makgwane PR, Hlekelele L, Motaung DE, Mavuso MA, Mphahlele-Makgwane MM, Mokoena TP. Recent advancement in the development of metal oxide heterostructures for environmental remediation. Metal Oxide-Based Heterostructures: Elsevier; 2023. p. 193-246.
18. Al-Mutairi SM, Al-Harbi MH. Water Production Management Strategy in North Uthmaniyah Area, Saudi Arabia. All Days; 2006/06/12: SPE; 2006.
19. Al-jaberi A, Saheb HM, Sadaka MWM, Abokehella AS, Al-Obeidi AH, Abed SH. Plasmon-Enhanced Visible Light Photocatalysis Using CuO/Ag/ZnO/Mn_2O_3 Nanocomposites for Efficient Organic Pollutant Degradation. Plasmonics. 2025;20(8):6463-6476.
20. Industrial Water Usage and Wastewater Treatment/Reuse. Green Chemistry and Chemical Engineering: CRC Press; 2016. p. 145-197.
21. Ortiz Rabell G, Juárez-Ramírez I, Alfaro Cruz MR. Bimetallic systems of ZnO/Al/Ag applied on cell PEC and photocatalytic system. Journal of Physics and Chemistry of Solids. 2023;181:111487.
22. Mandal P, Yadav MK, Majumder A, Ghosal PS. Application of nanomaterials synthesized using agriculture waste for wastewater treatment. Green and Sustainable Approaches Using Wastes for the Production of Multifunctional Nanomaterials: Elsevier; 2024. p. 305-318.
23. Saeed M, Al-Keridis LA, Khattak S, Alshuraym L, Alshammari N, Al-Amrah H, et al. Green Synthesis of Zinc Oxide Nanoparticles Using Egg White and Coriander Root Waste: Characterization and Anti-Cancer Efficacy in Hela Cells. Waste and Biomass Valorization. 2023;15(10):5639-5655.
24. Zhang S, Guo S, Li A, Liu D, Sun H, Zhao F. Low-cost bauxite residue-MoS2 possessing adsorption and photocatalysis ability for removing organic pollutants in wastewater. Sep Purif Technol. 2022;283:120144.
25. Tanuj, Kumar R, Kumar S, Kalra N, Sharma S, Singh A. Green synthesis of zinc oxide nanoparticles from Rhododendron arboreum extract and their potential applications in photocatalytic degradation of cationic dyes malachite green and Fuchsin basic dye. Chemical Papers. 2023;77(11):6583-6604.
26. Experimental and First-Principles Study of an Optimized Cylindrical-Shaped ZnO/gC_3N_4 Heterojunction for Enhanced Adsorption and Photocatalytic Degradation of Methylene Blue Dye. American Chemical Society (ACS). http://dx.doi.org/10.1021/acsomega.4c10430.s001
27. Moradi M, Rouhani M, Hekmati M, Veisi H, Esmaeli D. Green synthesis of gold nanoparticles supported over the Myrtus communis L extract modified magnetic iron oxide as a novel antibacterial agent. Results in Chemistry. 2025;15:102323.
28. A. Naser J, A. Himdan T, J. Ibraheim A. Adsorption Kinetic of Malachite Green Dye from Aqueous Solutions by Electrospun Nanofiber Mat. Oriental Journal of Chemistry. 2017;33(6):3121-3129.
29. Gupta S, Choudhary DK, Sundaram S. Green Synthesis and Characterization of Silver Nanoparticles Using Citrus sinensis (Orange peel) Extract and Their Antidiabetic, Antioxidant, Antimicrobial and Anticancer Activity. Waste and Biomass Valorization. 2024;16(3):1101-1114.
30. Umaralikhan L, Jaffar MJM. Green synthesis of ZnO and Mg doped ZnO nanoparticles, and its optical properties. Journal of Materials Science: Materials in Electronics. 2017;28(11):7677-7685.
31. Synthesis, Characterization, Adsorption Isotherm and Kinetic Study of Oil Palm Trunk-Derived Activated Carbon for Tannin Removal from Aqueous Solution. American Chemical Society (ACS).
32. Gilbert B, Ono RK, Ching KA, Kim CS. The effects of nanoparticle aggregation processes on aggregate structure and metal uptake. Journal of Colloid and Interface Science. 2009;339(2):285-295.
33. Weber WJ, Morris JC. Kinetics of Adsorption on Carbon from Solution. Journal of the Sanitary Engineering Division. 1963;89(2):31-59.
34. Weng C-H, Pan Y-F. Adsorption of a cationic dye (methylene blue) onto spent activated clay. J Hazard Mater. 2007;144(1-2):355-362.
35. Hu Y, Guo T, Ye X, Li Q, Guo M, Liu H, et al. Dye adsorption by resins: Effect of ionic strength on hydrophobic and electrostatic interactions. Chem Eng J. 2013;228:392-397.
36. Al-Ghouti MA, Da'ana DA. Guidelines for the use and interpretation of adsorption isotherm models: A review. J Hazard Mater. 2020;393:122383.
37. Thabede PM, Shooto ND, Xaba T, Naidoo EB. Adsorption studies of toxic cadmium(II) and chromium(VI) ions from aqueous solution by activated black cumin (Nigella sativa) seeds. Journal of Environmental Chemical Engineering. 2020;8(4):104045.
38. Chapter 2 Removal of heavy metals using mineral-based adsorbents. Heavy Metals Adsorption: De Gruyter; 2022. p. 17-62.
39. Al-Ghouti MA, Yousef I, Ahmad R, Ghrair AM, Al-Maaitah AA. Characterization of diethyl ether adsorption on activated carbon using a novel adsorption refrigerator. Chem Eng J. 2010;162(1):234-241.
40. Liu Y. Is the Free Energy Change of Adsorption Correctly Calculated? Journal of Chemical and Engineering Data. 2009;54(7):1981-1985.